Técnicas Computacionales en Ingeniería Civil - Curso 2020-21
Ejercicio 2

Diseño elástico no-lineal de pórticos metálicos con uniones semirígidas

José A. González Pérez

12 de enero de 2021

1. Plazo de entrega

Hasta el día 4 de febrero de 2021 inclusive. La práctica es **estrictamente individual** y el resultado se subirá a la plataforma de Enseñanza Virtual dentro del plazo de entrega establecido.

2. Enunciado

El ejercicio consiste en implementar un elemento viga bidimensional elástico lineal, como el representado en la Figura 1, que incluye dos muelles rotacionales en sus extremos que sirven para modelar la relación momento-rotación no-lineal asociada a la unión semirrígida de los extremos de la viga con los pilares de la estructura.

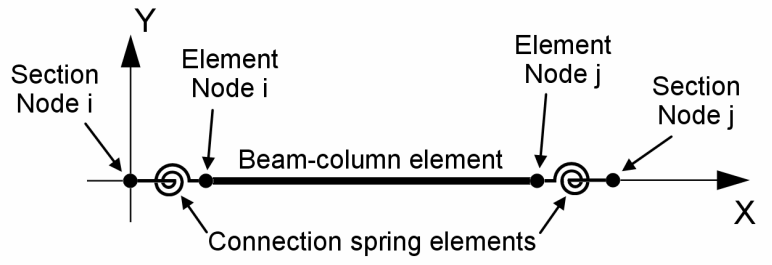

Figura 1: Esquema del elemento viga bidimensional con rigidez rotacional no-lineal en sus extremos.

Para cada elemento, supondremos que los muelles rotacionales ubicados en los dos nodos (i,j) son iguales y que la relación momento-rotación de la unión se puede expresar en la forma:

$$\theta_r = c_1(\kappa M) + c_2(\kappa M)^3 + c_3(\kappa M)^5$$

donde los coeficientes κ, c_1, c_2, c_3 dependerán del tipo de unión considerada. Además del efecto no-lineal de las uniones semirrígidas, se incluirá el efecto P-Δ en el elemento de forma simplificada, tal y como se describe en [1] y [2].

Tanto las propiedades del acero, como los datos geométricos de la sección del perfil y las constantes que definen el comportamiento de la unión, vendrán definidas en la variable *material*, tal y como se muestra en el listado 1. Utilizaremos también un punto de estado del material *element-state* en el elemento, que servirá únicamente para almacenar el estado interno de las uniones del perfil.

Listing 1: Ejemplo de definición un elemento barra bidimensional junto con con un material que define las propiedades del perfil y de las uniones de la viga..

```
clear all; close all; clc;

% Example:
data.node = [0  0; 1  0 ];
data.element = [1  2];

% Element
data.etype = 'Beam2D';
data.ndofnode = 3;

% Material properties (connection)
data.material.type = 'Connection2D';
data.material.kappa = 1;
data.material.c1 = 3.66e-4;
data.material.c2 = 1.15e-6;
data.material.c3 = 4.57e-8;

% Material properties (beam)
data.material.E = 2.1e6;
data.material.I = 0.0001;
data.material.A = 0.1;
```

El elemento barra bidimiensional cuenta con seis grados de libertad en el vector $\mathbf{d}^e$; desplazamiento horizontal, vertical y giro en cada nodo del elemento. De la misma manera, el vector de fuerzas internas del elemento $\mathbf{p}^e_{int}$ contará con seis componentes correspondientes a los esfuerzos axil, cortante y flector, ordenados de la

siguiente forma:

$$\mathbf{d}^e = \begin{Bmatrix} u_i \\ v_i \\ \theta_i \\ u_j \\ v_j \\ \theta_j \end{Bmatrix}, \qquad \mathbf{p}^e_{int} = \begin{Bmatrix} N_i \\ V_i \\ M_i \\ N_j \\ V_j \\ M_j \end{Bmatrix}, \qquad \mathbf{K}^e_T\left(\mathbf{d}^e\right) = \frac{\partial \mathbf{p}^e_{int}}{\partial \mathbf{d}^e}$$

donde la matriz de rigidez tangente elemental $\mathbf{K}^e_T$ resulta ser no-lineal debido a la contribución de las uniones semirrígidas y la consideración linealizada del efecto P-Δ. Deberemos por tanto implementar las funciones *peBeam2D.m*, *KeBeam2D.m* y *SeBeam2D.m*, junto la función del material *Connection2D.m*, que utilizaremos para resolver el problema mediante el método de Newton-Raphson.

Para probar el correcto funcionamiento del elemento, resolveremos la estructura metálica de la Figura 2 extraída de la referencia [1], para el caso concreto de uniones semirrígidas mediante piezas angulares atornilladas al alma (uniones tipo 1). Para ello, emplearemos los mismos perfiles definidos en la Tabla 4, junto con las dimensiones para las uniones recogidas en la Tabla 2 de la misma referencia.

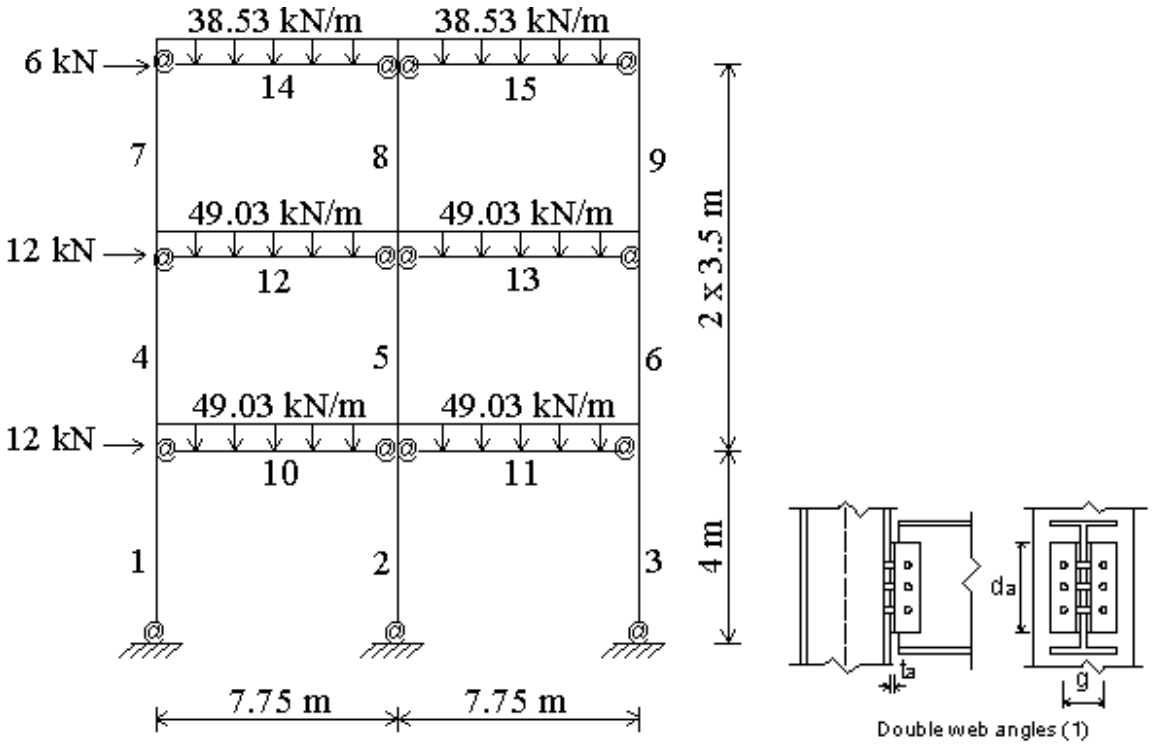

Figura 2: Descripción de la geometría de la estructura, acciones y numeración de los elementos (izquierda). Unión viga-pilar semirrígida mediante piezas angulares atornilladas al alma (derecha).

3. Formato de la memoria

La memoria del ejercicio debe de incluir los siguientes resultados:

1. Deducción de la expresión analítica del vector de fuerzas internas $\mathbf{p}^e_{int}$ del elemento incluyendo el efecto P-Δ.
2. Deducción de la expresión analítica de la matriz de rigidez tangente $\mathbf{K}^e_T$ del elemento incluyendo el efecto P-Δ.
3. Resolución del caso práctico propuesto.
4. Comparación de los resultados obtenidos en las uniones con los de la Tabla 7 de [1].
5. Representación de los diagramas momento-rotación de las uniones izquierda de la viga 10 y de la base de la columna 1.

4. Entrega

Finalmente, se subirá a Enseñanza Virtual el resultado en una carpeta comprimida en formato zip que contenga:

1. Memoria en formato pdf.
2. Código Matlab empleado para resolver el problema planteado.

Referencias

1. S. O. Degertekin, M. S. Hayalioglu. *Design of non-linear semi-rigid steel frames with semi-rigid column bases*, Electronic Journal of Structural Engineering, 4:1-16, (2004).
2. A. Chajes, J. E. Churchill. *Nonlinear frame analysis by finite element methods*, ASCE J. Struct. Eng., 113:1221-1235, (1987).

Design of non-linear semi-rigid steel frames with semi-rigid column bases

S. O. Degertekin
Civil Engineering Department, Dicle University, Muhendislik-Mimarlik Fakultesi
21280 Diyarbakir, Turkey

M. S. Hayalioglu
Civil Engineering Department, Dicle University, Muhendislik-Mimarlik Fakultesi
21280 Diyarbakir, Turkey

ABSTRACT

This article presents an analysis and design method for steel frames with semi-rigid connections and semi-rigid column bases. The analysis takes into account both the non-linear behaviour of beam-to-column connections and P-Δ effects of beam-column members. The Frye and Morris polynomial model is used for modelling of semi-rigid connections. The members are designed according to the specifications of American Institute of Steel Construction (AISC) Allowable Stress Design (ASD). The design process is interactive, and gives choices to the designer, to change member cross-sections and connection parameters for economical and practical reasons, interacting with computer. Two design examples with various type of connections are presented to demonstrate the efficiency of the method. The semi-rigid connection modelling yields more economical solutions than rigid connection modelling.The semi-rigid column base modelling also results in lighter frames. It is also shown that changes in the stiffness of the connections may result in economical solutions and alteration in the sways of the frames.

KEYWORDS
Allowable stress design; Non-linear analysis; Semi-rigid connections; Steel design; Unbraced frame;Semi-rigid column base

1 Introduction

Beam-to-column connections are assumed either perfectly pinned or fully rigid in most design of steel frames. This simplification leads to an incorrect estimation of frame behaviour. In fact, the connections are between the two extreme assumptions and possess some rotational stiffness. Full scale testing requires so as explaining the real behaviour of these connections. Bolted and welded beam-to-column connections rotate at an angle due to applied bending moment. This connection deformation has negative effect on frame stability, as it increases drift of the frame and causes a decrease in effective stiffness of the member, which is connected to the joint. An increase in frame drift will multiply the second-order (P-Δ) effects of beam-column members and thus will affect the overall stability of the frame. Hence, the non-linear features of beam-to-column connections have important function in structural steel design. As a result of experimental works done by several researchers, various semi-rigid connection modelling and their moment-rotation relationships are proposed. The main of these are linear, polynomial, cubic B spline, power and exponential models [1]. Some important research works have been reported for the analysis and design of semi-rigid frames [1-4].

AISC-ASD specification [5] describes three types of steel construction: rigid-frame, simple framing (unrestrained) and semi-rigid framing (partially restrained). This specification requires that the connections of the type of partially restrained construction have a flexibility

intermediate in degree between the rigidity of Type 1 and the flexibility of Type 2, and this type of construction may necessitate non-elastic (non-linear) deformations of structural steel parts. On the other hand, Eurocode 3 [6] proposes three types connection: rigid; semi-rigid and normally pinned or flexible. Eurocode 3 gives clear demarcation lines with exact values among these types.

The aim of the present study is also to consider both semi-rigid beam-to-column connections and semi-rigid column bases in the design of steel frames according to the specifications of AISC-ASD and thus to account the non-linear behaviour due to connection characteristics and P-Δ effects of beam-column members. A polynomial model proposed by Frye and Morris [7] is adopted as semi-rigid connection model. In the present study, a computer-based analysis and design method is developed which is interactive in character, and allows the designer to change member sizes and connection parameters to search satisfactory designs. The effect of changes in connection stiffness on the design results is investigated. The design results of frames with semi-rigid column bases are also compared with those of frames with rigid bases.

2 Connection modelling

A connection rotates through angle θ_r caused by applied moment M. This is the angle between beam and column from their original position. Several moment-rotation relationships have been derived from experimental studies for modelling semi-rigid connections of steel frames. These relationships vary from linear model to exponential models and are non-linear in nature. Relative moment-rotation curves of extensively used semi-rigid connections are shown in Fig.1 [8]. The geometry and size parameters of six types of connections are shown in Fig.2 [8]. In the present work, a polynomial model offered by Frye and Morris [7] is used because of its easy application. This model is expressed by an odd power polynomial which is in the following form:

$$\theta_r = c_1(\kappa M)^1 + c_2(\kappa M)^3 + c_3(\kappa M)^5 \quad (1)$$

where κ is standardization constant depends upon connection type and geometry; c_1, c_2, c_3 are the curve fitting constants. The values of these constants are given in Table 1 [9].

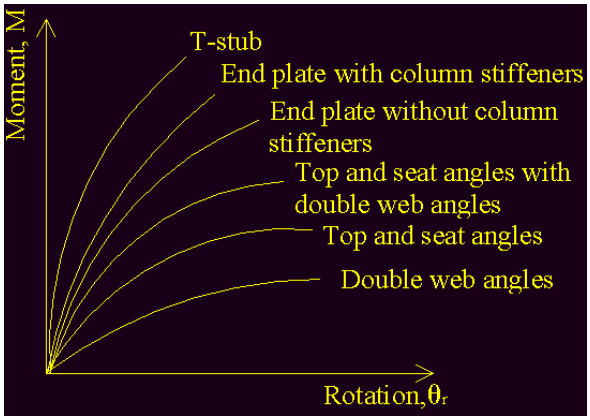

Fig. 1 - Moment-rotation curves of semi-rigid connections

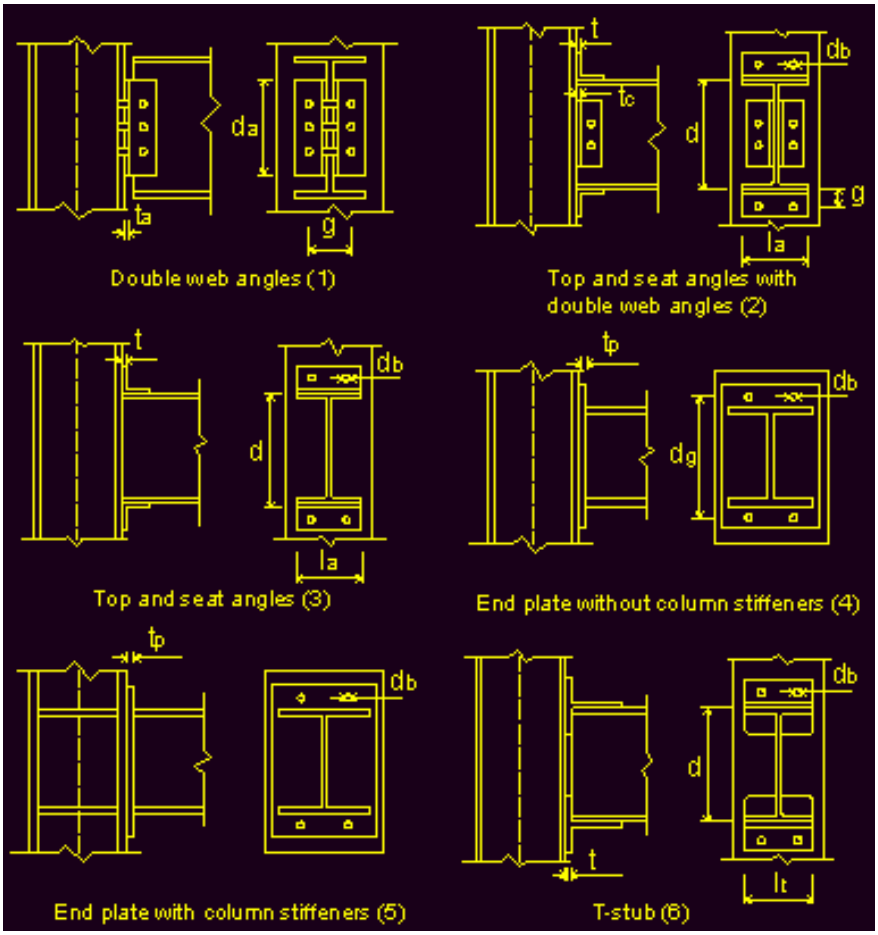

Fig. 2 - Semi-rigid connection types and size parameters (type-numbers are given in brackets)

Table 1 - Curve fitting constants and standardization constants for the Frye-Morris polynomial model

Connection types	Curve fitting constants	Standardization constants
1	$c_1=3.66\times10^{-4}$ $c_2=1.15\times10^{-6}$ $c_3=4.57\times10^{-8}$	$\kappa = d_a^{-2.4} t_a^{-1.81} g^{0.15}$
2	$c_1=2.23\times10^{-5}$ $c_2=1.85\times10^{-8}$ $c_3=3.19\times10^{-12}$	$\kappa = d^{-1.287} t^{-1.128} t_c^{-0.415} l_a^{-0.694} g^{1.35}$
3	$c_1=8.46\times10^{-4}$ $c_2=1.01\times10^{-4}$ $c_3=1.24\times10^{-8}$	$\kappa = d^{-1.5} t^{-0.5} l_a^{-0.7} d_b^{-1.5}$
4	$c_1=1.83\times10^{-3}$ $c_2=1.04\times10^{-4}$ $c_3=6.38\times10^{-6}$	$\kappa = d_g^{-2.4} t_p^{-0.4} d_b^{-1.5}$
5	$c_1=1.79\times10^{-3}$ $c_2=1.76\times10^{-4}$ $c_3=2.04\times10^{-4}$	$\kappa = d_g^{-2.4} t_p^{-0.6}$
6	$c_1=2.10\times10^{-4}$ $c_2=6.20\times10^{-6}$ $c_3=-7.60\times10^{-9}$	$\kappa = d^{-1.5} t^{-0.5} l_t^{-0.7} d_b^{-1.1}$

3 Analysis of steel frames with semi-rigid connections

The design procedure requires that the displacements and stresses in the frame system be known. This is achieved through a non-linear analysis of the steel frame. The non-linear analysis of steel frames takes into account both the geometrical non-linearity of beam-column members and non-linearity due to end connection flexibility of beam members. The columns of frames are generally continuous and do not have any internal flexible connections. However, the beams possess semi-rigid end connections, but have small axial forces with a geometric non-linearity of little importance. In the present study, three types of members are adopted for easiness in the design of steel frames with semi-rigid connections:

1. Beam-column member: A plane-frame member modified to include geometric non-linearity effect (P-Δ effect).

2. Beam member with semi-rigid end connections: A plane-frame member modified to incorporate end connection flexibility.

3. Beam-column member with semi-rigid column base: A bottom storey column modified to include semi-rigid base.

End forces and end displacements of a plane-frame member in member (local) coordinates are shown in Fig.3.

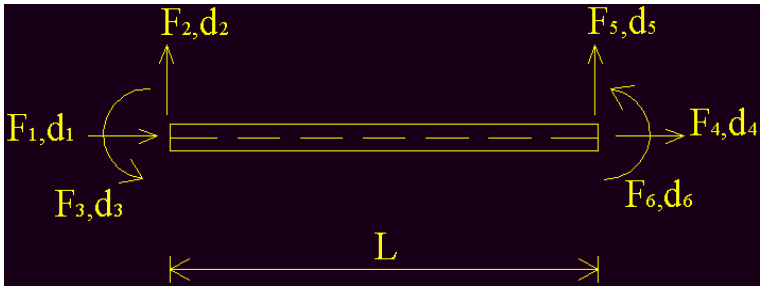

Fig. 3 - A plane-frame member with end forces and displacements

3.1 Beam-column member

The stiffness matrix of a beam-column member i in member (local) coordinates incorporating P-Δ effect can be expressed as follow:

$$[\bar{k}]_i = [k_E]_i + [k_p]_i \tag{2}$$

where $[k_E]_i$ is conventional linear-elastic stiffness matrix and $[k_p]_i$ is 'geometrical stiffness matrix' given as [10]

$$[k_p]_i = \frac{P}{L}\begin{bmatrix} 0 & & & & & \\ 0 & \frac{6}{5} & & & & \\ 0 & \frac{L}{10} & \frac{2L^2}{15} & & & \\ 0 & 0 & 0 & 0 & & \\ 0 & \frac{-6}{5} & -\frac{L}{10} & 0 & \frac{6}{5} & \\ 0 & \frac{L}{10} & \frac{-L^2}{30} & 0 & \frac{-L}{10} & \frac{2L^2}{15} \end{bmatrix} \tag{3}$$

where L is member length and P is the axial force in the member.

3.2 Beam member with semi-rigid end connections

Semi-rigid end connections of a beam can be represented by rotational springs as shown in Fig.4. θ_{rA} and θ_{rB} are the relative spring rotations of both ends and k_A and k_B are the corresponding spring stiffness expressed as:

$$k_A = \frac{M_A}{\theta_{rA}} \tag{4}$$

$$k_B = \frac{M_B}{\theta_{rB}} \tag{5}$$

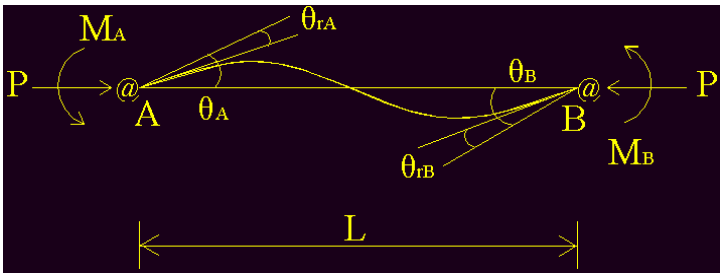

Fig. 4 - Beam member with rotational springs

The relationship between end-moments and end-rotations of a beam can be written by replacing the end-rotations θ_A and θ_B by $(\theta_A-\theta_{rA})$ and $(\theta_B-\theta_{rB})$ respectively, as follows:

$$M_A = \frac{EI}{L}\left[4\left(\theta_A - \frac{M_A}{k_A}\right) + 2\left(\theta_B - \frac{M_B}{k_B}\right)\right] \tag{6a}$$

$$M_B = \frac{EI}{L}\left[4\left(\theta_B - \frac{M_B}{k_B}\right) + 2\left(\theta_A - \frac{M_A}{k_A}\right)\right] \tag{6b}$$

where E is the modulus of elasticity and I is moment of inertia of the member. The Eqns. (6a) and (6b) can be expressed in the following form:

$$M_A = \frac{EI}{L}\left(r_{ii}\theta_A + r_{ij}\theta_B\right) \tag{7a}$$

$$M_B = \frac{EI}{L}\left(r_{ij}\theta_A + r_{jj}\theta_B\right) \tag{7b}$$

$$r_{ii} = \frac{1}{k_R}\left(4 + \frac{12EI}{Lk_B}\right) \tag{8a}$$

$$r_{jj} = \frac{1}{k_R}\left(4 + \frac{12EI}{Lk_A}\right) \tag{8b}$$

$$r_{ij} = \frac{2}{k_R} \tag{8c}$$

$$k_R = \left(1 + \frac{4EI}{Lk_A}\right)\left(1 + \frac{4EI}{Lk_B}\right) - \left(\frac{EI}{L}\right)^2\left(\frac{4}{k_A k_B}\right) \tag{8d}$$

Eqns. (7) are converted to the following stiffness matrix of a semi-rigid beam member with 6 degrees of freedom in local coordinates [11].

$$[k]_i = \begin{bmatrix} \frac{AE}{L} & & & & & \\ 0 & \left(r_{ii} + 2r_{ij} + r_{jj}\right)\frac{EI}{L^3} & & & & \\ 0 & \left(r_{ii} + r_{ij}\right)\frac{EI}{L^2} & r_{ii}\frac{EI}{L} & & & \\ \frac{-AE}{L} & 0 & 0 & \frac{AE}{L} & & \\ 0 & -\left(r_{ii} + 2r_{ij} + r_{jj}\right)\frac{EI}{L^3} & -\left(r_{ii} + r_{ij}\right)\frac{EI}{L^2} & 0 & \left(r_{ii} + 2r_{ij} + r_{jj}\right)\frac{EI}{L^3} & \\ 0 & \left(r_{ij} + r_{jj}\right)\frac{EI}{L^2} & r_{ij}\frac{EI}{L} & 0 & -\left(r_{ij} + r_{jj}\right)\frac{EI}{L^2} & r_{jj}\frac{EI}{L} \end{bmatrix} \tag{9}$$

where A is cross-sectional area of the member. Applying the known steps of the matrix displacement method, this matrix is obtained in global or structure coordinates for each member and structure stiffness matrix is constituted. The relationships between end-forces and end-displacements are also constructed according to the method. In the present work fixed-end forces which are derived in [2] are used for the beam members with semi-rigid end connections.

3.3 Beam-column member with semi-rigid column base

A column base with four bolt connection arrangements has been adopted as shown in Fig.5. The rotational stiffness of semi-rigid column base is given by Hensman and Nethercot [12] as

$$k_{base} = \frac{Ez^2 t}{20} \tag{10}$$

in which

$$z = r_b + \frac{H_c}{2} - \frac{t_f}{2} \tag{11}$$

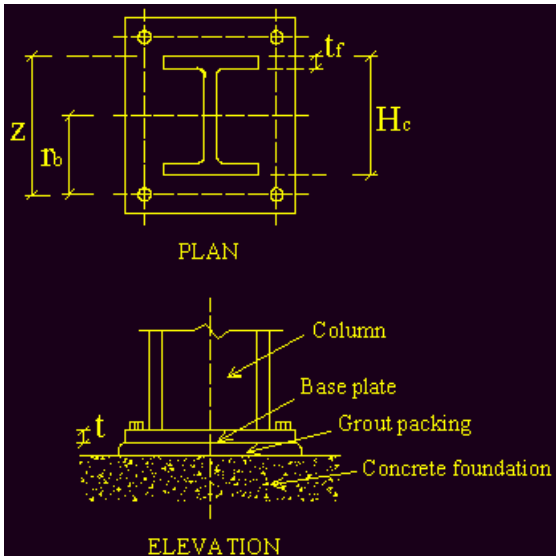

Fig. 5 - Simple semi-rigid column base detail

A linear spring model is used at the column feet; the rotations developed at the column base under serviceability load levels are assumed sufficiently small for use of the initial linear response to be sensible. The stiffness matrix of a beam-column member with semi-rigid column base is obtained by adding the matrices in Eqn. (2) and Eqn. (9) and replacing zero and k_{base} instead of $1/k_B$ and k_A respectively in the elements of the final matrix (the A end of the column is assumed to be column base).

3.4 Analysis procedure

The structure stiffness matrix is constructed by superimposing the member stiffness matrices contain geometric non-linearity and connection flexibility effects. This matrix is substituted in the structural equilibrium equations, which are non-linear and necessitate an iterative solution procedure. The applied loads are divided into a number of small-load increments and structural equilibrium equations are written in the incremental form:

$$[S]\{\Delta D\} = \{\Delta F\} \tag{12}$$

where $[S]$ is structure stiffness matrix, $\{\Delta F\}$ is incremental load vector, and $\{\Delta D\}$ is incremental displacement vector. The incremental Eqns.(12) are iteratively solved by a sequence of linear steps. The secant stiffness approach [10] is utilized for calculating the connection stiffness. The connection secant stiffness, SE, is defined as:

$$SE = \frac{\Delta M}{\Delta \theta_r} \tag{13}$$

where ΔM is the change in end moment during a load increment, $\Delta \theta_r$ is the change in relative spring rotation during the load increment. For each load increment, structure stiffness matrix is formed at the start of each iterative cycle. This requires calculation of the connection secant stiffness at the beginning of each cycle, and changing of the latest geometry and member end forces based on information from previous cycle. The convergent connection secant stiffness related to all load increments are shown in Fig.6. Convergence is obtained when the difference between joint displacements of two consecutive cycles falls below a specified tolerance.

A convergent solution of a load increment forms initial values for the next iteration and the iterative procedure goes on until all load increments are taken into account. The solutions for all load increments are added up to acquire a total non-linear response.

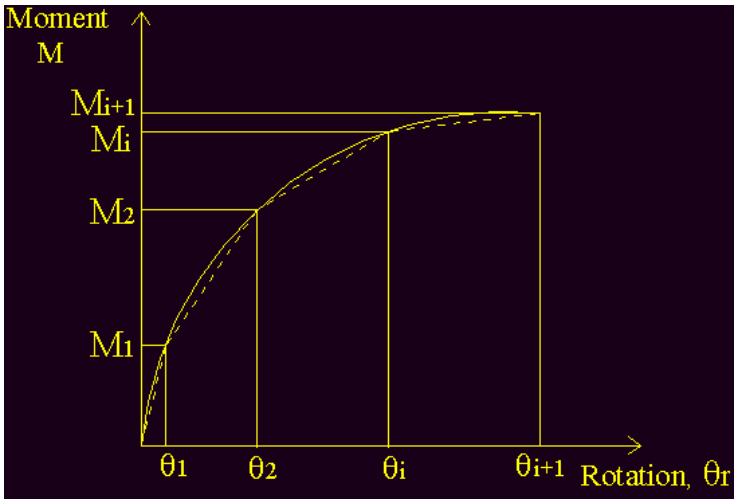

Fig. 6 - Connection secant stiffness through load increments

The above mentioned analysis procedure can be summarized through the following steps:

1. Divide applied loads into a series of small increments.

2. Carry out the linear analysis under first load increment and obtain the response of the frame, which is an initial estimate for the non-linear analysis.

3. Set up the member stiffness matrices $[k]_i$ and $[\bar{k}]_i$ for all members and assemble them in structure stiffness matrix $[S]$.

4. Solve the Eq. (12) for $\{\Delta D\}$ and then determine the incremental member end forces.

5. Obtain the connection secant stiffness by Eqn. (13).

6. Update the terms in the member stiffness matrices using the latest connection secant stiffness, and member forces. Update also structure geometry.

7. Repeat steps 3-6 until convergence is attained.

8. Calculate accumulated displacements and member end forces at convergence.

9. Continue the analysis with new load increments until all load increments are considered.

4 Design requirements

The interaction equations for the members of a steel frame under bending and axial stresses are of the form [5]:

For members subjected to both axial compression and bending stresses:

$$\frac{f_a}{F_a} + \frac{C_{mx} f_{bx}}{\left(1 - \frac{f_a}{F'_{ex}}\right) F_{bx}} \leq 1.0 \qquad (14)$$

$$\frac{f_a}{0.6F_y} + \frac{f_{bx}}{F_{bx}} \le 1.0 \tag{15}$$

When $f_a / F_a \le 0.15$, Eq. (16) is permitted in lieu of Eqs. (14) and (15).

$$\frac{f_a}{F_a} + \frac{f_{bx}}{F_{bx}} \le 1.0 \tag{16}$$

For members subjected to both axial tension and bending stresses:

$$\frac{f_a}{F_t} + \frac{f_{bx}}{F_{bx}} \le 1.0 \tag{17}$$

In Eqs. (14)-(17), the subscript x, combined with subscripts b, m and e indicates the axis of bending about which a particular stress or design property applies. In Eqs. (14)-(16), F_a is axial compressive stress permitted in the existence of axial force alone, F_{bx} is compressive bending stress permitted in the existence of bending moment alone, F'_{ex} is Euler stress divided by a factor of safety, f_a is computed axial compressive stress, f_{bx} is computed compressive bending stress at the point under consideration, C_{mx} is a coefficient whose value is taken as 0.85 for compression members in unbraced frames, F_y is the yield stress of steel. In Eq. (17), f_a is the computed axial tensile stress, f_{bx} is computed bending tensile stress, F_{bx} is allowable bending stress which is equal to $0.66F_y$ and F_t is the governing allowable tensile stress. $F_a, F_{bx}, 0.60F_y, F'_{ex}$ and F_t are increased 1/3 in accordance with the specification when produced by wind or earthquake acting alone or in combination with the design dead and live loads. Definitions of the permitted and Euler stresses and other details are given in AISC-ASD specifications [5]

The computed stresses are determined from non-linear analysis of steel frames under dead and live loads in combination with wind or earthquake loads.

4.1 Effective column-length factor

Effective length factor (K-factor) of columns must be estimated to evaluate the stability of columns in frames with rigid and semi-rigid connections. The factor K is required to determine the permitted axial compressive stress F_a and Euler stress F'_{ex} in the design of frame members. The effective length factor K for the columns in an unbraced frame is determined from the following interaction equation [13].

$$\frac{G_A G_B (\pi / K)^2 - 36}{6(G_A + G_B)} = \frac{\pi / K}{\tan(\pi / K)} \tag{18}$$

where G_A and G_B are relative stiffness factors for A-th and B-th ends of columns and given as:

$$G = \frac{\sum I_c / L_c}{\sum I_g / L_g} \tag{19}$$

where the summation is taken over all members connected to the joint, and where I_c is moment of inertia of column section corresponding to plane of buckling, L_c is unbraced length of

column, I_g is moment of inertia of beam/girder corresponding to plane of bending, and L_g is unbraced length of beam/girder .

In Eq.(18), it is assumed that the beams and girders are rigidly connected to columns at the joints. The beam/girder stiffness I_g/L_g in Eq.(19) is multiplied by the following factors to consider for different end connections:

The factor is 0.5 for far ends fixed; 0.67 for pinned, and $1/(1+6EI/L\times k)$ for flexibly connected, where k is spring stiffness of corresponding end.

5 Design procedure

Interacting with the computer, a design engineer can select member size founded on the value of interaction ratio given by Eqns. (14)-(17) compared with 1. An interaction ratio value greater than 1 implies that the member is insufficient and a larger section should be selected. Interaction ratios value smaller than 0.9 gives the implication that the design may be improved by selecting a reduced section. The engineer can also select and change interactively connection type and its size parameters to obtain adequate designs. The iterative and interactive design goes on until the engineer is convinced of his member and connection parameter selection.

The steps of the design of steel frames with semi-rigid connections are given in the following.

1. Assign the initial sections to the members of the frame from a specified list of standard sections and carry out the non-linear analysis of the frame under the applied loads by considering for non-linear behaviour of the semi-rigid connections and P-Δ effect.

2. Compute the member stresses using the member forces obtained from the non-linear analysis.

3. Check all members to satisfy the design requirements in Eqs.(14)-(17).

4. If the design is not satisfactory for any member, change the member size from the list for the insufficient or oversized member. Meanwhile, try various connection size parameters to achieve economic designs and control frame sway.

5. Repeat the procedure until satisfactory design is obtained.

6 Design examples

A computer program has been developed in the present study, which is implementation of the design procedure. Two design examples are presented to demonstrate the application of the design algorithm. The designs of semi-rigid frames are compared to the designs of rigid frames under the same design requirements. The designs of rigid frames are performed considering P-Δ effect of beam-column members. The material is grade A36 steel with a modulus of elasticity of 200000 MPa and yield stress of 248.2 MPa. Material density is 7850 kg/m^3. AISC (W) shapes are used as steel sections in all design examples considered in the present study. The numbers of semi-rigid connection types used in the designs are the same as the ones given in Fig.2.

6.1 Three-storey, two-bay frame

The dimensions, loading and numbering of members of three-storey two-bay frame are shown in Fig.7. The connection size parameters, which remain fixed during the design process, are given in Table 2 depending on the connection types.

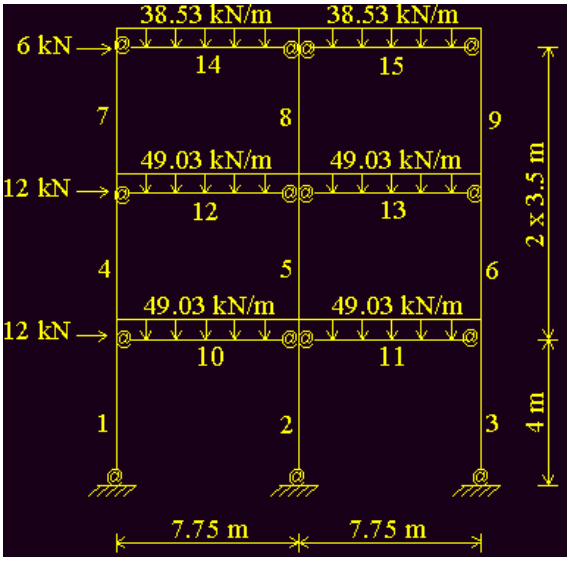

Fig. 7 - Three-storey, two-bay frame

Table 2 - The fixed connection size parameters for three-storey, two-bay frame

Connection Type	Connection size parameters (cm)
1	t_a =2.54 g =22.86
2	t =2.54 t_c =2.54 g =11.43
3	t =2.54 d_b =2.54
4	t_p =2.54 d_b =2.54
5	t_p =2.54 d_b =2.54
6	t =2.223 d_b =2.54

Table 3 - Final design results of 3-storey, two-bay frame. (Frame weights and sways)

Semi-rigid connection types	Weight (kg)		Top storey sway (cm)	
	Semi-rigid connection	Rigid connection	Semi-rigid connection	Rigid connection
1	6797	6196	1.13	0.71
2	5728		0.79	
3	7413		1.16	
4	5976		1.00	
5	5976		1.00	
6	5778		0.83	

The results of the final designs for six types of semi-rigid connections and also rigid connection are given in Table 3 in the form of frame weight and top storey sway. 3.5-7.6 % lighter frames with the connection types of 2,4,5,6 and 9.7-19.7% heavier frames with the connection types of 1,3 are obtained when compared to rigidly connected frame. Top storey sway of semi-rigid

frames increase by 12-64% over the sway of the rigidly connected frame. The final design sections and their maximum interaction ratio values for the six types of connection are presented in Table 4 and Table 5 respectively.

Table 4 - Final design sections for 3-storey, two-bay frame

Member no	Semi-rigid connection type						Rigid connection
	(1)	(2)	(3)	(4)	(5)	(6)	
1,4,7	W12×19	W12×19	W12×22	W12×19	W12×19	W12×22	W12×40
2,5,8	W12×40	W12×40	W12×40	W12×40	W12×40	W12×40	W12×40
3,6,9	W12×19	W12×26	W12×19	W12×22	W12×22	W12×26	W12×40
10-13	W12×87	W12×65	W12×96	W12×72	W12×72	W12×65	W12×65
14,15	W12×65	W12×58	W12×72	W12×58	W12×58	W12×58	W12×53

Table 5 - Maximum interaction ratio values for 3-storey, two-bay frame

Member no	Semi-rigid connection type						Rigid connection
	(1)	(2)	(3)	(4)	(5)	(6)	
1,4,7	1.000	0.991	0.909	0.932	0.932	0.936	0.883
2,5,8	0.905	0.903	0.896	0.910	0.911	0.906	0.907
3,6,9	1.000	0.992	0.986	0.974	0.980	0.978	0.930
10-13	0.974	0.978	0.940	1.000	1.000	0.892	0.926
14,15	0.981	0.936	0.860	0.993	0.987	0.865	0.998

For the final design of frame with connection type 2, the positive span-moments of the beam members are presented in Table 6 while the absolute maximum end-moments of the members are given in Table 7 . The results of Table 6 and Table 7 show that, in the frame with semi-rigid connections, the absolute maximum end-moments of beams decrease while the span moments of beams increase when compared to those of rigid frame. However, in the semi-rigid frame the overall maximum moments decrease in columns while they increase in small amount in most of the beams when compared to those of rigid frame.

Table 6 - Span moments in the beams of 3-storey, two-bay frame

Member no.	Semi-rigid connection Moment (kN-m)	Rigid connection Moment (kN-m)
10	282.42	142.95
11	277.18	138.09
12	278.86	135.55
13	275.40	133.89
14	223.80	115.25
15	220.57	114.23

Table 7 - Absolute maximum end-moments in 3-storey two-bay frame

Member no.	Semi-rigid connection Moment (kN-m)	Rigid connection Moment (kN-m)
1	11.08	60.40
2	27.70	25.72
3	42.28	88.55
4	32.99	106.94
5	17.16	16.30
6	47.35	118.63
7	39.31	131.48
8	4.96	6.80
9	50.10	139.28
10	130.04	288.15
11	92.64	253.79
12	116.38	267.66
13	98.22	247.02
14	92.76	219.83
15	87.80	213.03

6.2 Ten-storey, single-bay frame

Fig.8 shows configuration, dimensions, loading, and numbering of members. The fixed connection size parameters are presented in Table 8. The results of the final designs for six types of semi-rigid connections together with rigid connection are presented in Table 9 in the shape of weight and the sway of the top storey. 1.4-4.3 % lighter frames with the connection types of 1,2,4,5,6 are obtained in comparison with the rigidly connected frame. Semi-rigid frame drifts increase by 46-86 % over the rigid frame's sway.

The final design sections and their maximum interaction ratio values for the frame with type 4 connections together with the values for the rigid frame are given in Table 10.

Table 8 - The fixed connection size parameters for ten-storey, single-bay frame

Connection Type	**Connection size parameters (cm)**
1	t_a **=2.22** g **=15.24**
2	t **=1.91** t_c **=1.91** g **=6.35**
3	t **=2.54** d_b **=2.54**
4	t_p **=1.75** d_b **=2.54**
5	t_p **=1.75** d_b **=2.54**
6	t **=1.75** d_b **=2.22**

Table 9 - Final design results of ten-storey, single-bay frame. (Frame weights and sways)

Semi-rigid connection types	Weight (kg)		Top storey sway (cm)	
	Semi-rigid connection	Rigid connection	Semi-rigid connection	Rigid connection
1	11202	11542	13.46	9.12
2	11048		13.28	
3	12621		17.01	
4	11202		13.92	
5	11377		13.92	
6	11213		15.04	

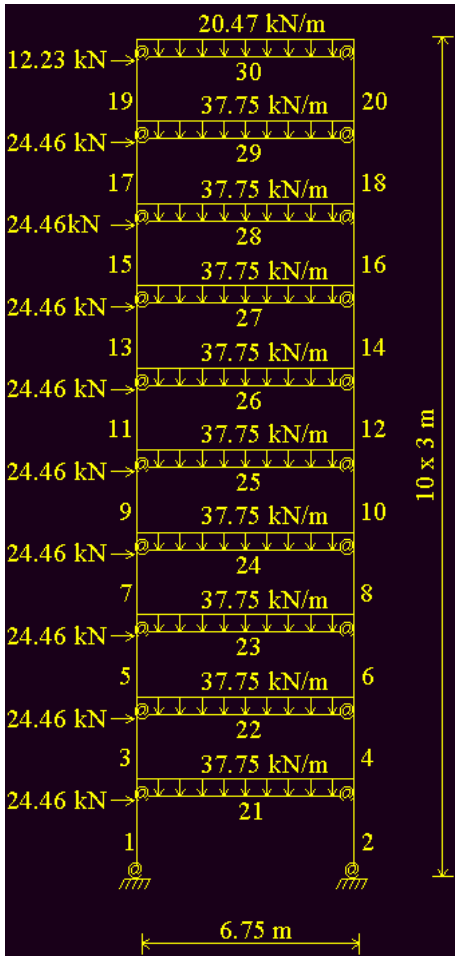

Fig. 8 - Ten-storey, single-bay frame

To examine the effect of the connection stiffness on the design of frames, the same frame with connection type 4 is designed with various connection size parameters and the results are presented in Table 11 in the form of frame weights and sways. The results of Table 11 indicate that, reducing of connection stiffness causes increase in both frame weight and sway.

The semi-rigid frames with rigid column bases are also designed and results are given in Table 12. According to these results the weights of frames with semi-rigid column bases decrease by 0.7-6.8% over the weights of frames with rigid bases depending on connection types. The semi-

rigid column bases also cause increase in the sways by 0.3-23%.

Table 10 - Final design sections and their maximum interaction ratios for ten-storey, single-bay frame (for connection type 4)

Member no.	Semi-rigid connection		Rigid connection	
	Section	The ratio	Section	The ratio
1-4	W14×99	0.956	W14×99	1.000
5-8	W14×74	0.954	W14×82	0.920
9-12	W12×58	0.923	W12×65	0.950
13-16	W14×34	0.940	W14×43	0.958
17-20	W12×19	0.892	W12×26	0.999
21-23	W21×57	0.875	W21×68	0.912
24-26	W18×65	1.000	W18×60	0.961
27-29	W18×60	0.987	W18×50	0.978
30	W18×65	0.917	W18×55	0.986

Table 11. The effect of connection stiffness on the design of ten-storey, single-bay frame

Connection size parameters (cm)	**Weight (kg)**	**Top storey sway (Cm)**
t_p **=2.540**	**11202**	**13.42**
t_p **=1.746**	**12172**	**13.97**
t_p **=1.588**	**12258**	**15.74**
t_p **=1.270**	**12293**	**19.00**
t_p **=0.792**	**12809**	**26.23**

Table 12 -Design results of ten-storey, single-bay frame for rigid column bases

Semi-rigid connection types	Weight (kg)	Top storey sway (cm)
1	11379	12.62
2	11225	12.43
3	12711	16.96
4	12024	12.32
5	12028	12.68
6	11717	12.25

7 Discussion and conclusions

A combined analysis and design procedure is presented for the design of steel frames with semi-rigid connections and semi-rigid column bases accounting non-linear behaviour of frames. Computer-based analysis and design procedure is interactive and iterative in nature. Design examples are included to demonstrate the influence of connection flexibility and geometric non-linearity on the design of steel frames.

It is observed from the results of design examples that semi-rigid connection modelling may create lighter frames providing that appropriate connection size parameters are selected. The reduction in weight is calculated as 7.6% at most in the examples considered. The end moments of a beam with semi-rigid connections decrease while its span moment increases in comparison with those of the beam with rigid connections.

Connection stiffness plays important role in the design of semi-rigid frames. The semi-rigid connections cause a large increase in frame sway over the rigid connections. This increase is found to be up to 86% in the examples presented. Trying various connection stiffness values, the sway can be controlled and economic frames can be obtained. Reducing of connection stiffness results in increase in frame weight and sway. The reason for the increase in weights is that an increase in frame displacements magnifies column and beam end moments and thus larger sections are assigned to the members. The softening of connections results in considerable increase in frame sway. Examining the results of Table 11, it is found that the fifth trial for reducing the stiffness results in an increase in the sway by 95% over the first trial. An economic frame system can be attained by controlling frame sway with the stiffness of the connections.

In semi-rigid frames, semi-rigid column bases create lighter frames but they increase the sways when compared to the rigid base.

REFERENCES

1. Abdalla K.M., Chen W.F., “Expanded database of semi-rigid steel connections”, *Computer and Structures*, Vol. 56, No. 4, 1995, pp 553-564.
2. Dhillon B.S., and O’Malley J.W., “Interactive design of semirigid steel frames”, *Journal of Structural Engineering* - ASCE, Vol. 125, No. 5, May 1999, pp 556-564.
3. Kim Y., and Chen W.F., “Practical analysis for partially restrained frame design”, *Journal of Structural Engineering* - ASCE, Vol. 124, No. 7, July 1998, pp 736-749.
4. Goto Y., and Miyashita S., “Classification system for rigid and semirigid connection”, *Journal of Structural Engineering* - ASCE, Vol. 124, No. 7, July 1998, pp 750-757.
5. American Institute of Steel Construction. Manual of steel construction, allowable stress design. Chicago,1989.
6. Eurocode 3. Design of Steel Structures. Part I: General rules and rules for buildings. Comite European de Normalisation (CEN) Brussels, Belgium, 1992.
7. Frye M.J., and Morris G.A., “Analysis of flexibly connected steel frames”, *Canadian Journal of Civil Engineering*, Vol. 2, 1975, pp 280-291.
8. Chen W.F., Goto Y., and Liew J.Y.R., “Stability Design of Semi-Rigid Frames”, John Wiley & Sons Inc., New York, 1996.
9. Faella C., Piluso, V. and Rizzano, G. “Structural Steel Semirigid Connections”, CRC Press LLC, Boca Raton, 2000.
10. Chajes, A. and Churcill, J.E. “Nonlinear Frame Analysis by Finite Element Methods”, *Journal of Structural Engineering*,-ASCE, Vol. 113, No. 6, June 1987, pp 1221-1235.
11. Chen, W.F., and Lui, E.M. “Stability Design of Steel Frames”, CRC Press, Inc., Boca Raton, 1991.
12. Hensmann, J.S., and Nethercot, D.A. “Numerical study of unbraced composite frames: generation of data to validate use of the wind moment method of design” *Journal of Constructional Steel Research*, Vol. 57, 2001, pp 791-809.
13. Kishi, N. Chen, W.F. and Goto, Y. “Effective length factor of columns in semirigid and unbraced frames”, *Journal of Structural Engineering* - ASCE, Vol. 123, No. 3, March 1997, pp 313-320.

Nonlinear Frame Analysis by Finite Element Methods

By Alexander Chajes,[1] M. ASCE, and James E. Churchill,[2] A. M. ASCE

Abstract: A review of the basic concepts involved when constructing nonlinear load-deflection curves of framed structures by the finite element method is presented. The study is limited to the geometrically nonlinear behavior of elastic structures. Three different procedures are considered: the linear incremental method, the nonlinear incremental method, and the direct method. For each method the governing equations are derived, and the procedure used to plot the load-deflection curve is outlined.

Introduction

In recent years it has become apparent that the solution of a stability problem usually involves not only the determination of the critical load but also the construction of the nonlinear load-deflection curve for the actual structure. At present, a sizeable number of papers exist that present procedures for using the finite-element method to construct such nonlinear load-deflection curves (1,2,3,4,7,8). However, due to the relative complexity of these methods and due to the existence of many minor as well as major variations among the different procedures, it is extremely difficult to obtain a clear picture of the fundamentals from the existing publications. It is therefore the aim of this paper to elucidate the basic concepts involved in the construction of nonlinear load-deflection curves by the finite element method. The material presented here is limited to nonlinear behavior of elastic framed structures.

Geometrically nonlinear problems are sometimes referred to as large-deflection problems. Such problems do not necessarily differ from linear or small-deflection problems because large deflections literally occur, but rather because axial stresses exist that in the presence of lateral displacements exert a significant influence on the stiffness of the structure. In comparison with linear problems, for which the terms constituting the stiffness matrix of the system are constant, the stiffness matrix for geometrically nonlinear problems contains terms that are functions of the deformation of the structure. In other words, the stiffness matrix $[K]$ that relates the forces $[F]$ to the displacements $[D]$ in the equation $[K][D] = [F]$ must, for a geometrically nonlinear problem, be written with respect to a deformed geometry that is not known in advance. The different ways in which this equation can be set up and solved is the main concern of this paper.

Basically, there are three procedures for obtaining the load-deflection curve for a geometrically nonlinear problem: the linear incremental method, the nonlinear incremental method, and the direct method.

[1]Prof., Civ. Engrg. Dept., Univ. of Massachusetts, Amherst, MA 01003.
[2]Res. Asst., Civ. Engrg. Dept., Univ. of Massachusetts, Amherst, MA.

Note.—Discussion open until November 1, 1987. To extend the closing date one month, a written request must be filed with the ASCE Manager of Journals. The manuscript for this paper was submitted for review and possible publication on February 6, 1986. This paper is part of the *Journal of Structural Engineering*, Vol. 113, No. 6, June, 1987. ©ASCE, ISSN 0733-9445/87/0006-1221/$01.00. Paper No. 21554.

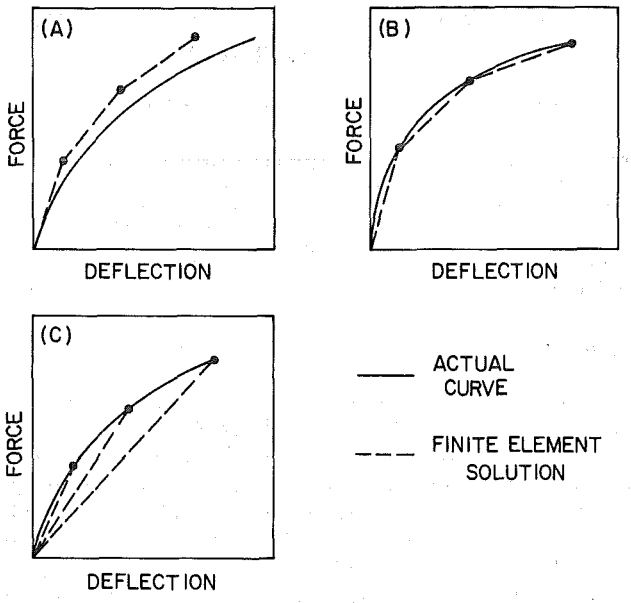

FIG. 1.—(*a*) Linear Incremental Method; (*b*) Nonlinear Incremental Method; and (*c*) Direct Method

In the linear incremental method, the nonlinear load-deflection curve is constructed by employing a stepwise linear procedure. The load is applied as a series of small increments, and for each of these increments the change in the deformation is determined using a linear analysis. A so-called tangent stiffness matrix, based on the geometry and internal forces existing at the beginning of any step, is used to calculate the change in the deformation caused by the load increment, i.e., $[K_T][\Delta D] = [\Delta F]$. The total displacements and internal forces existing at the end of any step are obtained by summing the incremental changes in displacements and internal forces up to that point.

The nonlinear incremental method is similar to the linear incremental method in that both apply the load as a series of small increments and then calculate the change in the displacements caused by each load increment. The difference between the two methods is in the way they determine the incremental displacements. The linear incremental method employs a tangent stiffness matrix based on the internal forces and deformations existing at the beginning of the load step to obtain the incremental displacements. Since the terms of this stiffness matrix remain constant for a given load step, a single calculation suffices to give the incremental displacements for that load step. By comparison, the nonlinear incremental method employs an incremental stiffness matrix that is a function of the internal forces and displacements developed during the load step as well as those existing at the beginning of the load step. This stiffness matrix can obviously not be evaluated at the beginning of the load step. Instead, an iteration scheme is employed to continuously

update the stiffness matrix as better and better approximations of the incremental deformations are calculated.

The manner in which each of the two incremental methods approximates the actual load-deflection curve is shown in Figs. 1(*a*) and 1(*b*). It is evident that the numerical solution tends to drift away from the exact solution for the linear incremental method. This procedure, therefore, requires smaller load steps than those needed when using the nonlinear incremental method.

In the direct method, the deformation corresponding to any load along the load-deflection curve is obtained by applying the entire load in a single step. This method thus deals with total deformations and total loads as compared to the incremental methods that deal with incremental deformations and incremental loads. The direct method can be used to obtain the deformation corresponding to a single value of the load, or the procedure can be repeated for ever increasing values of the load and thus be used to plot the entire load-deflection curve as shown in Fig. 1(*c*). In this method the desired deformations are related to the applied load by a so-called secant stiffness matrix, i.e., $[K_S][D] = [F]$. Since $[K_S]$ depends on the internal forces and deformations that exist when the total load is acting, and since these quantities are not known at the beginning of the calculation, the terms in $[K_S]$ must be determined by iteration. In this aspect the method resembles the nonlinear incremental method.

Theory

The principle of stationary potential energy provides a convenient way for developing the force-deflection relationship for a structural element. The total potential energy V of the element is given by

$$V = U - \sum_{i=1}^{n} f_i d_i \quad \ldots\ldots (1)$$

in which U = the strain energy; and f_i and d_i = the element nodal forces and displacements. If the strain energy is expressed as a function of the nodal displacements, Eq. 1 can be rewritten in matrix form as

$$V = \frac{1}{2}[d]^T[k][d] - [d]^T[f] \quad \ldots\ldots (2)$$

in which $[k]$ = the element stiffness matrix. Taking the derivative of V with respect to the nodal displacements and setting the resulting expression equal to zero gives

$$[k][d] = [f] \quad \ldots\ldots (3)$$

which is the desired force-displacement relation.

In the following sections, the principle of stationary potential energy will be used to develop several different forms of Eq. 3.

Incremental Stiffness Matrix.—Using a procedure developed by Martin (5,6), the incremental stiffness matrix of a beam-column element will now be obtained. The element is assumed to have length L, cross-sec-

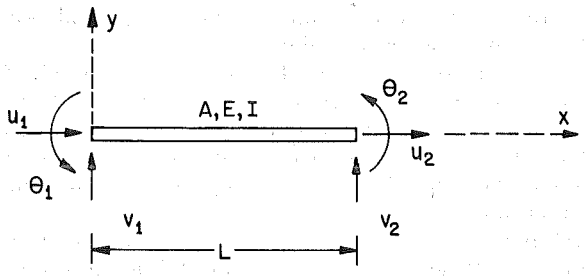

FIG. 2.—Beam-Column Element

tional area A, moment of inertia I, modulus of elasticity E, and the six nodal displacements $[d]$ and forces $[f]$ defined in Fig. 2.

To obtain the relationship between an incremental change in the element deformations and the corresponding incremental change in the forces, let ϵ_0 be the axial strain in the element at the beginning of the incremental step, and let ϵ_a be the additional strain that develops during the step. The change in the strain energy for the step is then given by

$$U = \int_L \int_A \left[\int_{\epsilon_0}^{\epsilon_0+\epsilon_a} \sigma d\epsilon \right] dA dx \quad \ldots\ldots (4)$$

Making use of Hooke's Law and integrating with respect to ϵ one obtains

$$U = E\epsilon_0 \int_L \int_A \epsilon_a dA dx + \frac{E}{2} \int_L \int_A \epsilon_a^2 dA dx \quad \ldots\ldots (5)$$

The strain-displacement relation for a beam-column element is

$$\epsilon_a = \frac{du}{dx} + \frac{1}{2}\left(\frac{dv}{dx}\right)^2 - y\frac{d^2v}{dx^2} \quad \ldots\ldots (6)$$

Since ϵ_a is the change in strain, u and v in Eq. 6 represent the corresponding changes in the displacements and not the total displacements.

Substituting Eq. 6 into Eq. 5 and integrating over the cross-sectional area, leads to

$$U = P \int_0^L \left[\frac{du}{dx} + \frac{1}{2}\left(\frac{dv}{dx}\right)^2\right] dx + \frac{E}{2} \int_0^L \left[A\left(\frac{du}{dx}\right)^2 + I\left(\frac{d^2v}{dx^2}\right)^2 + A\frac{du}{dx}\left(\frac{dv}{dx}\right)^2 + \frac{A}{4}\left(\frac{dv}{dx}\right)^4\right] dx \quad \ldots\ldots (7)$$

in which $P = \epsilon_0 EA$ is the axial force that exists in the element at the beginning of the incremental step.

In order to transform U into a function of the nodal displacements, it is first necessary to express u and v in terms of the nodal dispalcements. Toward this end the following displacement functions are assumed:

$$u = a_0 + a_1 x; \quad v = b_0 + b_1 x + b_2 x^2 + b_3 x^3 \quad \ldots\ldots (8)$$

Using the boundary conditions at the ends of the element gives

$$u = \left(1 - \frac{x}{L}\right) u_1 + \left(\frac{x}{L}\right) u_2; \quad v = \left(1 - \frac{3x^2}{L^2} + \frac{2x^3}{L^3}\right) v_1$$

$$+ \left(\frac{3x^2}{L^2} - \frac{2x^3}{L^3}\right) v_2 + \left(-\frac{2x^2}{L} + x + \frac{x^3}{L^2}\right) \theta_1 + \left(-\frac{x^2}{L} + \frac{x^3}{L^2}\right) \theta_2 \quad \ldots\ldots\ldots (9)$$

It is now possible by substituting Eqs. 9 into Eq. 7 to express U in terms of the incremental nodal displacements ($u_1, v_1, \theta_1, u_2, v_2, \theta_2$). Once this has been accomplished, application of the principle of stationary potential energy leads to the expression

$$[k_I][\Delta d] = [\Delta f] \quad \ldots\ldots\ldots (10)$$

in which $[k_I]$ = the incremental stiffness matrix that relates the incremental element displacements $[\Delta d]$ to the corresponding incremental element forces $[\Delta f]$.

The incremental stiffness matrix in Eq. 10 consists of the sum of four distinct matrices. Thus

$$[k_I] = [k_0] + [k_P] + \frac{AE}{2}[k_1] + \frac{AE}{3}[k_2] \quad \ldots\ldots\ldots (11)$$

The terms that make up each of these matrices are given in Appendix I. The first matrix, $[k_0]$, is the conventional linear stiffness matrix for uncoupled bending and axial behavior. Its terms are constants that depend neither on the element forces nor on the displacements. By comparison, the terms of the second matrix, $[k_P]$, are linear functions of the axial force P present at the beginning of the incremental step. This matrix, commonly referred to as the initial stress matrix, gives a first order approximation of the interaction between the axial force and the transverse displacements. The remaining two matrices, $[k_1]$ and $[k_2]$, consist, respectively, of terms that are linear and quadratic functions of the incremental element displacements. These matrices account for the change that occurs in the axial force and transverse displacements during the incremental load step.

Tangent Stiffness Matrix.—In some instances, the nonlinear effects due to the change in element forces and deformations occurring during the incremental step are very small compared to the nonlinear effect of the forces and deformations that exist at the beginning of the step. When this is the case, $[k_1]$ and $[k_2]$ can be neglected and the stiffness matrix takes the form

$$[k_T] = [k_0] + [k_P] \quad \ldots\ldots\ldots (12)$$

Since this stiffness matrix depends only on the internal forces and deformations existing at the beginning of the load step, it is commonly referred to as the tangent stiffness matrix.

Secant Stiffness Matrix.—The secant stiffness matrix, which relates total displacements to total loads, may be obtained using the same procedure that was followed in the foregoing pages for determining the incremental stiffness matrix, except that the initial strain ϵ_0 is now set

equal to zero. Accordingly the strain energy given by Eq. 5 is replaced by

$$U = \frac{E}{2}\int_L\int_A (\epsilon_a)^2\, dA dx \quad \ldots\ldots (13)$$

in which ϵ_a = the total strain instead of the incremental strain.

As before, making use of the strain-displacement relation given by Eq. 6, one obtains

$$U = \frac{E}{2}\int_0^L \left[A\left(\frac{du}{dx}\right)^2 + I\left(\frac{d^2v}{dx^2}\right) + A\left(\frac{du}{dx}\right)\left(\frac{dv}{dx}\right)^2 + \frac{A}{4}\left(\frac{dv}{dx}\right)^4\right] dx \quad \ldots\ldots (14)$$

The terms u and v now represent total displacements and not incremental displacements as before. Finally, using the displacement functions given by Eqs. 8 and applying the principle of stationary potential energy, one obtains

$$[k_s][d] = [f] \quad \ldots\ldots (15)$$

in which $[k_s]$ = the element secant stiffness matrix that relates the total element displacements $[d]$ to the corresponding total element forces $[f]$.

The secant stiffness matrix in Eq. 15 consists of three matrices. Thus

$$[k_s] = [k_0] + \frac{AE}{2}[k_1] + \frac{AE}{3}[k_2] \quad \ldots\ldots (16)$$

As before, $[k_0]$ = the conventional linear stiffness matrix; and $[k_1]$ and $[k_2]$ are made up of terms that are linear and quadratic functions respectively of the element nodal displacements. The terms in these matrices are identical to the ones in the corresponding matrices defined by Eq. 11 and listed in Appendix I. The only difference is that the nodal displacements in the matrices making up $[k_s]$ are total displacements, whereas the same terms represent incremental displacements in the case of $[k_I]$.

Transformation Matrix.—To transform the stiffness matrices derived in the preceding sections from element to global coordinates, the transformation matrix $[T]$ given in Appendix II is used. The transformation is carried out using the relation

$$[K] = [T]^T [k][T] \quad \ldots\ldots (17)$$

in which $[K]$ = the element stiffness matrix in global coordinates; and $[k]$ = the element stiffness matrix in local coordinates. The form of $[T]$ is the same regardless of whether the incremental stiffness matrix is used in the incremental method or the secant stiffness matrix is used in the direct method. However, since the terms of $[T]$ correspond to the geometry at the beginning of the load step, they are determined using the initial undeformed geometry when applying the direct method, and the deformed geometry existing at the beginning of the load step when the incremental method is employed.

Solution Procedures

Linear Incremental Method.—The linear incremental method uses the stiffness matrix given by Eq. 12 to determine incremental displacements

corresponding to incremental loads. At the start of each load step, the existing deformed geometry and internal forces are used to form the stiffness matrix of the structure. The internal forces are employed to form $[k_p]$ and the deformed geometry to update $[T]$. In addition, the value of L in $[k_p]$ must be updated to account for changes in the member length. By comparison, the fact that the linear part of the deformation remains small allows one to keep L in $[k_0]$ constant at its original value. Incremental loads are then applied, and the equation $[K_T][\Delta D] = [\Delta F]$ is solved for the corresponding incremental displacements. The incremental displacements thus obtained are in turn used to calculate changes in the internal forces. New values of the total displacements and internal forces are then determined by adding the incremental quantities to the previously existing total values. These new internal forces and total displacements are now used to form the stiffness matrix for the next load increment.

One of the most important characteristics of the linear incremental procedure is that, for a given load step, $[K_T]$ is based solely on the deformations and internal forces existing at the beginning of that load step. Changes of the deformations and internal forces that occur during the load step are neglected. As a consequence, $[K_T]$ remains constant during the calculation of the incremental displacements, and a single solution of the equations suffices to obtain the desired results. On the other hand, since the procedure neglects the changes in the deformations and internal forces that take place during a load step, it is necessary to make the load steps relatively small. A summary of the linear incremental method is given in Appendix III.

Nonlinear Incremental Method.—The nonlinear incremental method employs the stiffness matrix given by Eq. 11. Since the terms in $[k_1]$ and $[k_2]$ are functions of the incremental displacements that occur during the load step, and since these quantities are not known at the beginning of the load step, an iterative scheme is required to obtain a solution. The first step in the procedure is identical to the linear incremental method. Using the deformed geometry and the internal forces existing at the beginning of the load step, $[k_0]$ and $[k_P]$ are formed, and $[k_1]$ and $[k_2]$ are set equal to zero. The matrix $[k_I] = [k_0] + [k_P]$ is then used to determine a first estimate of the incremental displacements for the given load step.

An iteration scheme is now employed in which the stiffness matrix is continuously updated using the previously calculated incremental displacements. $[k_0]$ and $[k_P]$ do not change during the iteration. The former consists only of constant terms, and the values of P and L in the latter are by definition the axial force and length existing at the beginning of the load step. Similarly, the transformation matrix $[T]$ remains constant during the iteration, being updated only at the beginning of a new load step. Thus $[k_1]$ and $[k_2]$ are the only parts of the stiffness matrix that change during the iteration process. They are continuously reformed using the previously calculated incremental displacements.

Although there are different ways of carrying out the iteration, the Newton-Raphson method appears to be the most widely accepted one. The procedure consists of determining the imbalances between the member forces and the external loads that exist at the nodes of the structure at the end of each iteration step. The force imbalances thus obtained

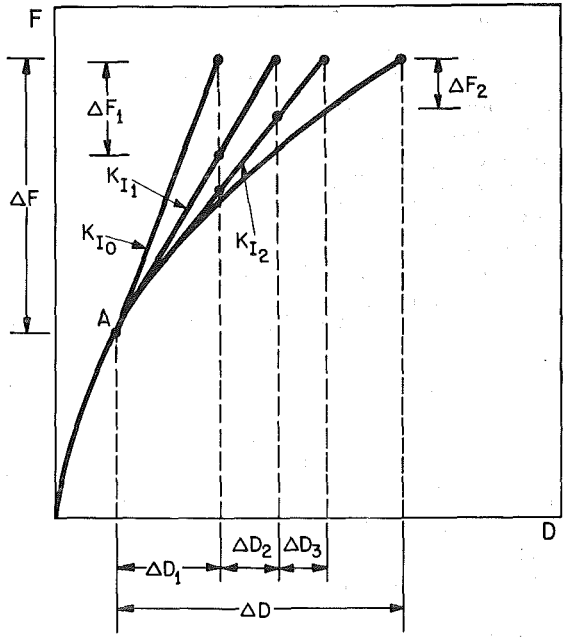

FIG. 3.—Iteration Procedure for Nonlinear Incremental Method

are then used to calculate corrections to the previously determined incremental displacements.

As an illustration, the procedure used to determine the incremental displacement $[\Delta D]$ corresponding to a load increment $[\Delta F]$ for the load-deflection curve depicted in Fig. 3 is outlined. In the initial step, the equation $[K_I]_0[\Delta D]_1 = [\Delta F]$ uses $[K_I]_0$, evaluated at point A, to determine $[\Delta D]_1$. Next, a revised stiffness matrix $[K_I]_1$, updated to account for $[\Delta D]_1$, is used in the equation $[K_I]_1[\Delta D]_1 = [\Delta F] - [\Delta F]_1$ to solve for the force imbalance $[\Delta F]_1$. The procedure is now repeated. First, the equation $[K_I]_1[\Delta D]_2 = [\Delta F]_1$ is used to determine $[\Delta D]_2$, corresponding to the load increment $[\Delta F]_1$. Then, using an updated stiffness matrix $[K_I]_2$, which accounts for $[\Delta D]_2$, the equation $[K_I]_2[\Delta D]_2 = [\Delta F] - [\Delta F]_2$ leads to the new load imbalance $[\Delta F]_2$. Thus, the recurrence relations used to solve for the incremental displacement $[\Delta D]_i$ and the force imbalance $[\Delta F]_i$ are respectively

$$[K_I]_{i-1}\,[\Delta D]_i = [\Delta F]_{i-1} \quad \ldots\ldots (18)$$

and $$[k_I]_i\,[\Delta D]_i = [\Delta F] - [\Delta F]_i \quad \ldots\ldots (19)$$

The incremental displacement used to form $[K_I]_i$ is given by

$$[\Delta D] = [\Delta D]_1 + [\Delta D]_2 + \ldots + [\Delta D]_i \quad \ldots\ldots (20)$$

Conversion is achieved when the force imbalance $[\Delta F]_i$ given by Eq. 19 becomes negligible. The sought-after incremental displacement $[\Delta D]$ is then given by Eq. 20.

The nonlinear incremental method is summarized in Appendix IV.

Direct Method.—The direct method uses the secant stiffness matrix given by Eq. 16 to determine total deflections produced by total loads. Whereas the load was applied as a series of increments in the incremental methods, the load is applied in a single step in the direct method. Since $[k_1]$ and $[k_2]$ are functions of the unknown displacements, an iteration procedure is required to solve Eq. 16 for the displacements corresponding to a given set of applied loads. Instead of the Newton-Raphson method used in the nonlinear incremental procedure, a straight iteration method is used here.

The iteration procedure is shown in Fig. 4. Starting with the undeformed structure, it is desirable to obtain the deflection $[D_A]$ corresponding to the load $[F_A]$. In the initial step, $[k_1]$ and $[k_2]$ are set equal to zero, and the remaining linear part of the stiffness matrix, $[k_0]$, is used to solve for the first estimate of the deflection $[D]_1$. Next, $[D]_1$ is used to evaluate $[k_1]$ and $[k_2]$, and the revised stiffness matrix, which now includes all three parts, is used to determine $[D]_2$. This procedure is repeated until the solution converges.

The recurrence relation used to obtain the deflection $[D]_i$ for any cycle i of the iteration process is

$$[K_S]_{i-1}[D]_i = [F] \quad \text{(21)}$$

Equilibrium can be checked after any step of the procedure by comparing the actual applied load $[F]$ with the resultant of the member forces given by $[F]_i = [K_S]_i\,[D]_i$.

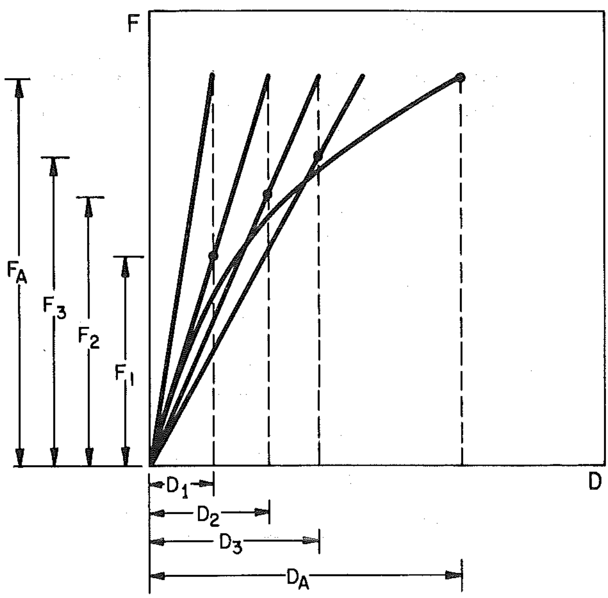

FIG. 4.—Iteration Procedure for Direct Method

Since the total load is applied to the original undeformed structure for each step of the iteration process, the transformation matrix $[T]$ is never updated. It is always based on the original undeformed geometry.

The direct method is outlined in Appendix V.

Conclusions

The basic concepts involved in the construction of load-deflection curves for geometrically nonlinear systems by the finite element method have been presented. Three procedures have been considered in detail. They are the linear incremental method, the nonlinear incremental method, and the direct method. For each method, the governing equations have been derived, and the procedure used to plot the load-deflection curve is outlined. In both the linear and nonlinear incremental methods, the load is applied in a series of small steps. The difference between the two methods is that the latter requires an iteration procedure whereas the former does not. However, the linear incremental method requires the use of smaller load increments than those necessitated by the nonlinear incremental method. In the direct method, the entire load corresponding to any point on the load-deflection curve is applied in a single step. This method also requires the use of an iteration procedure.

Acknowledgments

The work reported herein was supported partially by a grant from the Control Data Corporation.

Appendix I.—Stiffness Matrix Terms

In Eq. 11 the element stiffness matrix is expressed in the form $[k_I] = [k_0] + [k_P] + (AE/2)[k_1] + (AE/3)[k_2]$. The terms of making up the four submatrices of $[k_I]$ are as follows:

$$[k_0] = \begin{array}{c} \begin{matrix} u_1 & v_1 & \theta_1 & u_2 & v_2 & \theta_2 \end{matrix} \\ \begin{bmatrix} \frac{AE}{L} & 0 & 0 & -\frac{AE}{L} & 0 & 0 \\ 0 & \frac{12EI}{L^3} & \frac{6EI}{L^2} & 0 & -\frac{12EI}{L^3} & \frac{6EI}{L^2} \\ 0 & \frac{6EI}{L^2} & \frac{4EI}{L} & 0 & -\frac{6EI}{L^2} & \frac{2EI}{L} \\ -\frac{AE}{L} & 0 & 0 & \frac{AE}{L} & 0 & 0 \\ 0 & -\frac{12EI}{L^3} & -\frac{6EI}{L^2} & 0 & \frac{12EI}{L^3} & -\frac{6EI}{L^2} \\ 0 & \frac{6EI}{L^2} & \frac{2EI}{L} & 0 & -\frac{6EI}{L^2} & \frac{4EI}{L} \end{bmatrix} \begin{matrix} u_1 \\ v_1 \\ \theta_1 \\ u_2 \\ v_2 \\ \theta_2 \end{matrix} \end{array} \quad \ldots\ldots\ldots \quad (22)$$

$$[k_p] = \begin{matrix} \\ u_1 \\ v_1 \\ \theta_1 \\ u_2 \\ v_2 \\ \theta_2 \end{matrix} \begin{matrix} \begin{matrix} u_1 & v_1 & \theta_1 & u_2 & v_2 & \theta_2 \end{matrix} \\ \begin{bmatrix} 0 & 0 & 0 & 0 & 0 & 0 \\ 0 & \frac{6P}{5L} & \frac{P}{10} & 0 & -\frac{6P}{5L} & \frac{P}{10} \\ 0 & \frac{P}{10} & \frac{2PL}{15} & 0 & -\frac{P}{10} & -\frac{PL}{30} \\ 0 & 0 & 0 & 0 & 0 & 0 \\ 0 & -\frac{6P}{5L} & -\frac{P}{10} & 0 & \frac{6P}{5L} & -\frac{P}{10} \\ 0 & \frac{P}{10} & -\frac{PL}{30} & 0 & -\frac{P}{10} & \frac{2PL}{15} \end{bmatrix} \end{matrix} \quad \ldots\ldots (23)$$

In which P, the initial axial force, should be given a minus sign if the member is in compression.

The nonzero terms in $[k_1]$ and $[k_2]$ are

$$k_{1(1,2)} = k_{1(4,5)} = -k_{1(2,4)} = -k_{1(1,5)} = \frac{6}{5L^2}(v_2 - v_1) - \frac{1}{10L}(\theta_1 + \theta_2) \quad \ldots\ldots (24)$$

$$k_{1(1,3)} = k_{1(3,4)} = \frac{1}{10L}(v_2 - v_1) + \frac{1}{30}(\theta_2 - 4\theta_1) \quad \ldots\ldots (25)$$

$$k_{1(1,6)} = -k_{1(4,6)} = \frac{1}{10L}(v_2 - v_1) + \frac{1}{30}(\theta_1 - 4\theta_2) \quad \ldots\ldots (26)$$

$$k_{1(2,2)} = k_{1(5,5)} = -k_{1(2,5)} = \frac{6}{5L^2}(u_2 - u_1) \quad \ldots\ldots (27)$$

$$k_{1(3,3)} = k_{1(6,6)} = \frac{2}{15}(u_2 - u_1) \quad \ldots\ldots (28)$$

$$k_{1(3,6)} = -\frac{1}{30}(u_2 - u_1) \quad \ldots\ldots (29)$$

$$k_{1(3,5)} = k_{1(5,6)} = -k_{1(2,3)} = -k_{1(2,6)} = \frac{1}{10L}(u_2 - u_1) \quad \ldots\ldots (30)$$

$$k_{2(2,2)} = k_{2(5,5)} = -k_{2(2,5)}$$

$$= \frac{1}{140}\left[\frac{18\theta_1^2}{L} + \frac{18\theta_2^2}{L} + \frac{432}{L^3}(v_2 - v_1)^2 - \frac{108}{L^2}(v_2 - v_1)(\theta_1 + \theta_2)\right] \quad \ldots\ldots (31)$$

$$k_{2(2,3)} = -k_{2(3,5)} = \frac{1}{280}\left[-3\theta_1^2 + 3\theta_2^2 + 6\theta_1\theta_2 + \frac{108}{L^2}(v_2 - v_1)^2 - \frac{72}{L}\theta_1(v_2 - v_1)\right] \quad \ldots\ldots (32)$$

J. Struct. Eng. 1987.113:1221-1235.

$$k_{2,(2,6)} = k_{2(5,6)} = \frac{1}{280}\left[3\theta_1^2 - 3\theta_2^2 + 6\theta_1\theta_2 + \frac{108}{L^2}(v_2 - v_1)^2 - \frac{72}{L}\theta_2(v_2 - v_1)\right] \quad (33)$$

$$k_{2(3,3)} = \frac{1}{140}\left[12L\theta_1^2 + L\theta_2^2 - 3L\theta_1\theta_2 + \frac{18}{L}(v_2 - v_1)^2 + 3(v_2 - v_1)(\theta_1 - \theta_2)\right] \quad (34)$$

$$k_{2(3,6)} = \frac{1}{280}[-3L\theta_1^2 - 3L\theta_2^2 + 4L\theta_1\theta_2 - 6(v_2 - v_1)(\theta_1 + \theta_2)] \quad (35)$$

$$k_{2(6,6)} = \frac{1}{140}\left[L\theta_1^2 + 12L\theta_2^2 - 3L\theta_1\theta_2 + \frac{18}{L}(v_2 - v_1)^2 + 3(v_2 - v_1)(\theta_2 - \theta_1)\right] \quad (36)$$

Appendix II.—Transformation Matrix

$$[T] = \begin{bmatrix} \lambda & \mu & 0 & 0 & 0 & 0 \\ -\mu & \lambda & 0 & 0 & 0 & 0 \\ 0 & 0 & 1 & 0 & 0 & 0 \\ 0 & 0 & 0 & \lambda & \mu & 0 \\ 0 & 0 & 0 & -\mu & \lambda & 0 \\ 0 & 0 & 0 & 0 & 0 & 1 \end{bmatrix} \quad (37)$$

in which $\lambda = \cos\theta$; $\mu = \sin\theta$; and θ = the angle between the global and element coordinate axes.

Appendix III.—Summary of Linear Incremental Method

1. Form $[k_0]$ for each element.
2. Specify incremental loads $[\Delta F]$.
3. Using existing geometry and axial forces, form $[k_p]$ for each element and construct $[T]$.
4. Using the equation $[k_T] = [k_0] + [k_p]$, form element stiffness matrices.
5. Transform element stiffness matrices from local to global coordinates and combine to form global stiffness matrix $[K_T]$.
6. Solve for incremental displacements $[\Delta D]$ using the equations $[K_T][\Delta D] = [\Delta F]$.
7. Using $[\Delta D]$, determine change in axial forces $[\Delta P]$.
8. Calculate total values of $[D]$, $[P]$, and $[F]$ by adding increments to existing quantities.
9. Return to step 2 for next load increment.

J. Struct. Eng. 1987.113:1221-1235.

Appendix IV.—Summary of Nonlinear Incremental Method

1. Form $[k_0]$ for each element.
2. Specify incremental loads $[\Delta F]$.
3. Using existing geometry and axial forces, form $[k_p]$ for each element and construct $[T]$.
4. Using the equation $[k_I] = [k_0] + [k_p]$, form element stiffness matrices.
5. Transform element stiffness matrices from local to global coordinates and combine to form global stiffness matrix $[K_I]_0$.
6. Initialize i: $i = 0$.
7. Let $[\Delta F]_0 = [\Delta F]$.
8. Increment i: $i = i + 1$.
9. Solve for displacement $[\Delta D]_i$ using the equation $[K_I]_{i-1}[\Delta D]_i = [\Delta F]_{i-1}$.
10. Obtain $[\Delta D] = \Sigma_{n=1}^{i} [\Delta D]_n$.
11. Use $[\Delta D]$ to obtain $[\Delta d]$ and form $[k_1]$ and $[k_2]$.
12. Form element stiffness matrices using the equation $[k_I] = [k_0] + [k_P] + [k_1] + [k_2]$.
13. Transform element stiffness matrices from local to global coordinates and combine to form global stiffness matrix $[K_I]_i$.
14. Solve for the force imbalance $[\Delta F]_i$ using the equation $[K_I]_i [\Delta D]_i = [\Delta F] - [\Delta F]_i$.
15. Repeat steps 8–14 until $[\Delta F]_i$ becomes negligible.
16. Calculate total values of $[D]$, $[P]$, and $[F]$ by adding increments to existing quantities.
17. Return to step 2 for next load increment.

Appendix V.—Summary of Direct Method

1. Form $[k_0]$ for each element.
2. Use initial undeformed geometry to form $[T]$.
3. Let $[k_s] = [k_0]$ to obtain element stiffness matrices.
4. Transform element stiffness matrices from local to global coordinates and combine to form global stiffness matrix $[K_s]_0$.
5. Specify loads $[F]$.
6. Initialize i: $i = 0$.
7. Increment i: $i = i + 1$.
8. Solve for displacements $[D]_i$ using the equation $[K_s]_{i-1}[D]_i = [F]$.
9. Use $[D]_i$ to obtain $[d]$ and form $[k_1]$ and $[k_2]$.
10. Form the element stiffness matrices using the equation $[k_s] = [k_0] + [k_1] + [k_2]$.
11. Transform element stiffness matrices from local to global coordinates and combine to form global stiffness matrix $[K_s]_i$.
12. Solve for the resultant of the member forces at each joint using the equation $[F]_i = [K_s]_i[D]_i$.
13. Repeat steps 7–12 until $[F]_i = [F]$.
14. Return to step 5 for the next set of loads $[F]$.

Appendix VI.—References

1. Connor, J. J., Logcher, R. D., and Chan, S. C., "Nonlinear Analysis of Elastic Framed Structures," *Journal of the Structural Division*, ASCE, Vol. 94, No. 6, Jun., 1968, pp. 1525–1547.

2. Ebner, A. M,. and Ucciferro, J. J., "A Theoretical and Numerical Comparison of Elastic Nonlinear Finite Element Methods," *Computers and Structures*, Vol. 2, 1972, pp. 1043–1061.
3. Jennings, A., "Frame Analysis Including Change of Geometry," *Journal of the Structural Division*, ASCE, Vol. 94, No. 3, Mar., 1968, pp. 627–644.
4. Mallet, R. H., and Marcal, P. V., "Finite Element Analysis of Nonlinear Structures," *Journal of the Structural Division*, ASCE, Vol. 94, No. 9, Sep., 1968, pp. 2081–2105.
5. Martin, H. C., "Large Deflection and Stability Analysis by the Direct Stiffness Method," *Technical Report No. 32-931*, Jet Propulsion Laboratory, California Institute of Technology, Pasadena, Calif., 1966.
6. Martin, H. C., "On the Derivation of Stiffness Matrices for the Analysis of Large Deflection and Stability Problems," *Proceedings, Conference of Matrix Methods in Structural Mechanics*, Wright-Patterson Air Force Base, Ohio, Oct., 1965, pp. 697–716.
7. Powell, G. H., "Theory of Nonlinear Elastic Structures," *Journal of the Structural Division*, ASCE, Vol. 95, No. 12, Dec., 1969, pp. 2687–2701.
8. Wen, R. K., and Rahimzadeh, J., "Nonlinear Elastic Frame Analysis by Finite Element," *Journal of Structural Engineering*, ASCE, Vol. 109, No. 8, Aug., 1983, pp. 1952–1971.

APPENDIX VII.—NOTATION

The following symbols are used in this paper:

A = cross-sectional area;
a_0, a_1 = constants;
b_0, b_1, b_2, b_3 = constants;
$[D]$ = structure nodal displacements;
$[d]$ = element nodal displacements;
E = modulus of elasticity;
$[F]$ = structure nodal forces;
$[f]$ = element nodal forces;
I = moment of inertia;
$[K]$ = global stiffness matrix;
$[K_I], [K_S], [K_T]$ = instantaneous, secant, and tangent stiffness matrices in global coordinates;
$[k]$ = element stiffness matrix;
$[k_I], [k_S], [k_T]$ = instantaneous, secant, and tangent stiffness matrices in element coordinates;
$[k_P]$ = initial stress stiffness matrix;
$[k_0]$ = linear stiffness matrix;
$[k_1], [k_2]$ = nonlinear stiffness matrices;
L = length;
P = axial force;
$[T]$ = transformation matrix;
U = strain energy;
u, v = displacements in the x and y directions;
u_1, v_1, θ_1 = element nodal displacements at end 1 of the member;
u_2, v_2, θ_2 = element nodal displacements at end 2 of the member;
V = total potential energy;
x, y = coordinates;

ϵ = strain; and
σ = stress.

Subscripts

a = additional;
I = instantaneous;
S = secant;
T = tangent; and
0 = initial.

Superscripts

T = transpose of matrix.